Supplementary Fig. 1

Application of DD domains for inducible control of neuronal protein function.

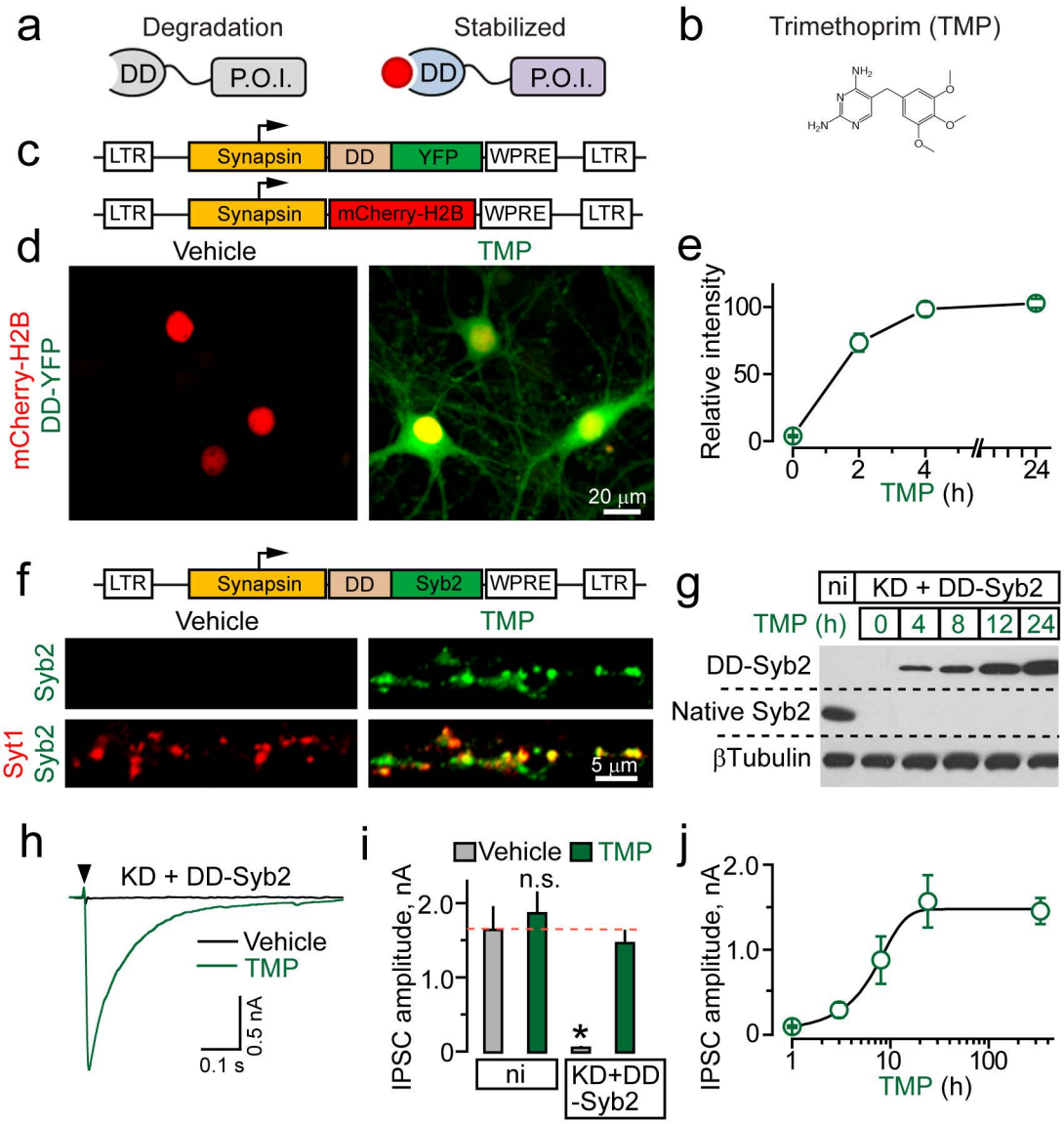

Supplementary Figure 1

a, Fusion proteins composed of a protein of interest (P.O.I.) and a mutant destabilizing form of ecDHFR (DD) undergo rapid degradation. DD-P.O.I.s are stabilized with the antibiotic Trimethoprim (TMP), which binds to DD tags with high affinity.

b, The structure of TMP.

c-j, Properties of DD-P.O.I.s introduced into cultured neurons with lentiviruses. Mixed cortical cultures were infected at 5 days after plating (5DIV) and analyzed at 14-15 DIV.

c, Schematic representation of viruses encoding DD-YFP and a constitutive pan-neuronal nuclear tracer, Cherry-H2B.

d, Typical images of control neurons co-infected with DD-YFP and Cherry-H2B, and neurons that were continuously treated with TMP (10 μM).

e, Time-course of DD-YFP stabilization. Averaged YFP fluorescent intensities are plotted as a function of time after addition of TMP to the culture medium (n=10 neurons).

f-j, Regulation of vesicular neurotransmitter release with DD-Syb2. Cultures were infected with a virus encoding shRNA against native Syb2 and shRNA-insensitive rescue DD-Syb2 cDNA (KD+DD-Syb2).

f, Representative images of nerve terminals before and 24 hours after TMP addition (10 μM). Synaptic boutons were visualized by labeling with antibodies to Syb2 (green) and Syt1 (red).

g, Time-course of DD-Syb2 stabilization. Non-infected (ni) and KD+DD-Syb2 neurons were probed by immunoblotting for Syb2 and βTubulin (as a loading control). Note a loss of native Syb2 and progressive TMP-dependent increase in the levels of DD-Syb2.

h, Representative traces of evoked inhibitory postsynaptic currents (IPSCs) monitored from KD+DD-Syb2 neurons in the presence of AMPA and NMDA receptor blockers, CNQX and APV. IPSCs were recorded in whole-cell mode before and 24 hours after TMP application.

i, Mean amplitudes of IPSCs sampled from non-treated non-infected and KD+DD-Syb2 neurons, and neurons that were treated for 24 hours with TMP. Note that stabilization of DD-Syb2 fully rescues synaptic transmission.

j, Temporal dynamics of rescue of neurotransmitter release by stabilized DD-Syb2. IPSCs were recorded at different time points after TMP addition. Data are from two independent culture preparations. See also Supplementary **Table 1.**

Supplementary Fig. 2

Nucleotide and protein sequences of ecDHFR-Cre (DD-Cre).

a. DD-Cre Nucleotide Sequence (5’-3’)

ATGATCTCTCTGATTGCCGCTCTGGCCGTGGACTACGTGATCGGGATGGAAAACGCTATGCCATGG
AATCTGCCCGCCGATCTGGCTTGGTTCAAGAGGAACACCCTGAACAAGCCAGTGATCATGGGCAGA
CACACTTGGGAGTCCATTGGCCGGCCCCTGCCTGGACGCAAGAACATCATTCTGAGCTCCCAGCC
CTCTACCGACGACAGGGTGACATGGGTGAAAAGTGTGGACGAAGCCATTGCCGCTTGCGGAGATG
TGCCCGAGATCATGGTCATCGGCGGAGGGAGAGTGATCGAGCAGTTCCTGCCTAAGGCCCAGAAA
CTGTACCTGACTCACATTGACGCTGAGGTGGAAGGGGACACCCATTTTCCTGATTATGAGCCAGAC
GATTGGGAAAGCGTGTTCTCCGAGTTTCACGACGCCGATGCTCAGAATTCTCATAGTTATTGCTTTG
AGATCCTGGAAAGGAGA*GGCGCGCCT*AAGAAGAAGAGGAAGGTGTCCAATTTACTGACCGTACACC
AAAATTTGCCTGCATTACCGGTCGATGCAACGAGTGATGAGGTTCGCAAGAACCTGATGGACATGTT
CAGGGATCGCCAGGCGTTTTCTGAGCATACCTGGAAAATGCTTCTGTCCGTTTGCCGGTCGTGGGC
GGCATGGTGCAAGTTGAATAACCGGAAATGGTTTCCCGCAGAACCTGAAGATGTTCGCGATTATCTT
CTATATCTTCAGGCGCGCGGTCTGGCAGTAAAAACTATCCAGCAACATTTGGGCCAGCTAAACATG
CTTCATCGTCGGTCCGGGCTGCCACGACCAAGTGACAGCAATGCTGTTTCACTGGTTATGCGGCGG
ATCCGAAAAGAAAACGTTGATGCCGGTGAACGTGCAAAACAGGCTCTAGCGTTCGAACGCACTGAT
TTCGACCAGGTTCGTTCACTCATGGAAAATAGCGATCGCTGCCAGGATATACGTAATCTGGCATTTC
TGGGGATTGCTTATAACACCCTGTTACGTATAGCCGAAATTGCCAGGATCAGGGTTAAAGATATCTC
ACGTACTGACGGTGGGAGAATGTTAATCCATATTGGCAGAACGAAAACGCTGGTTAGCACCGCAGG
TGTAGAGAAGGCACTTAGCCTGGGGGTAACTAAACTGGTCGAGCGATGGATTTCCGTCTCTGGTGT
AGCTGATGATCCGAATAACTACCTGTTTTGCCGGGTCAGAAAAAATGGTGTTGCCGCGCCATCTGC
CACCAGCCAGCTATCAACTCGCGCCCTGGAAGGGATTTTTGAAGCAACTCATCGATTGATTTACGG
CGCTAAGGATGACTCTGGTCAGAGATACCTGGCCTGGTCTGGACACAGTGCCCGTGTCGGAGCCG
CGCGAGATATGGCCCGCGCTGGAGTTTCAATACCGGAGATCATGCAAGCTGGTGGCTGGACCAAT
GTAAATATTGTCATGAACTATATCCGTAACCTGGATAGTGAAACAGGGGCAATGGTGCGCCTGCTG
GAAGATGGCGAT**TAG**

b. DD-Cre Amino Acid Sequence

MISLIAALAVDYVIGMENAMPWNLPADLAWFKRNTLNKPVIMGRHTWESIGRPLPGRKNIILSSQPSTDD
RVTWVKSVDEAIAACGDVPEIMVIGGGRVIEQFLPKAQKLYLTHIDAEVEGDTHFPDYEPDDWESVFSEF
HDADAQNSHSYCFEILERRGAPKKKRKVSNLLTVHQNLPALPVDATSDEVRKNLMDMFRDRQAFSEHT
WKMLLSVCRSWAAWCKLNNRKWFPAEPEDVRDYLLYLQARGLAVKTIQQHLGQLNMLHRRSGLPRPS
DSNAVSLVMRRIRKENVDAGERAKQALAFERTDFDQVRSLMENSDRCQDIRNLAFLGIAYNTLLRIAEIAR
IRVKDISRTDGGRMLIHIGRTKTLVSTAGVEKALSLGVTKLVERWISVSGVADDPNNYLFCRVRKNGVAA
PSATSQLSTRALEGIFEATHRLIYGAKDDSGQRYLAWSGHSARVGAARDMARAGVSIPEIMQAGGWTN
VNIVMNYIRNLDSETGAMVRLLEDGD@

Blue-ecDHFR
Black-linker
Green-Cre

Supplementary Fig. 3

Comparative analysis of DD-Cre and Cre-ERT2 *in vitro*.

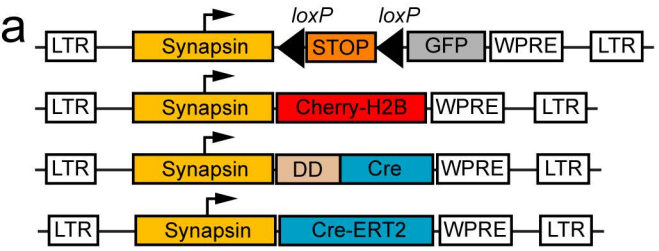

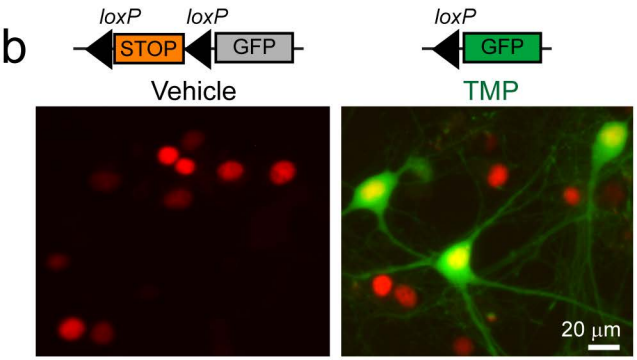

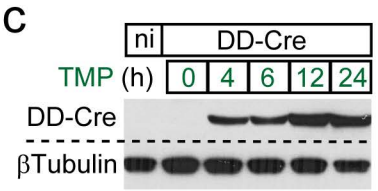

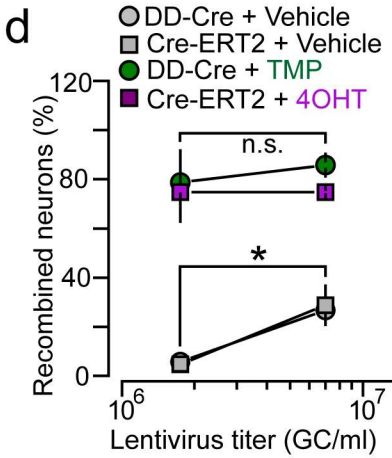

Supplementary Figure 3

Cultured cortical neurons were co-infected at 5 DIV with lentiviruses encoding a Cre-inducible fluorescent reporter, floxstop-GFP, a constitutive pan-neuronal tracer, Cherry-H2B, and either DD-Cre or Cre-ERT2. All constructs were driven by the Synapsin promoter. All measurements were performed at 15 DIV.

a, Schematic representation of lentivirus vectors.

b, TMP-dependent loxP recombination catalyzed by DD-Cre. Typical images show induction of Cre reporter in response to drug treatment (10 μM for 24 hours).

c, Biochemical analysis of the time-course of DD-Cre stabilization. Protein homogenates were examined by immunoblotting with antibodies to Cre and βTubulin (as a loading control).

d, Quantitative assessment of background and drug-dependent recombination mediated by DD-Cre and Cre-ERT2. Neurons were co-infected with floxstop-GFP, Cherry-H2B and corresponding Cre viruses of indicated titers. Subsequently, cells carrying DD-Cre or Cre-ERT2 were treated for 24 hours with TMP (10 μM) and 4OHT (2 μM), respectively. Vehicle-treated cultures were used as controls. Recombination efficiencies were calculated as ratios of GFP-positive cells to all neurons tagged with mCherry-H2B. Note that DD-Cre and Cre-ERT2 exhibit a similar dependence of background activity on copy numbers. Data from two culture preparations are represented as Mean±S.D. * = $p<0.05$ (determined by Students t-test). See also Supplementary **Table 1.**

Supplementary Fig. 4

Comparative analysis of DD-Cre and Cre-ERT2 *in vivo*.

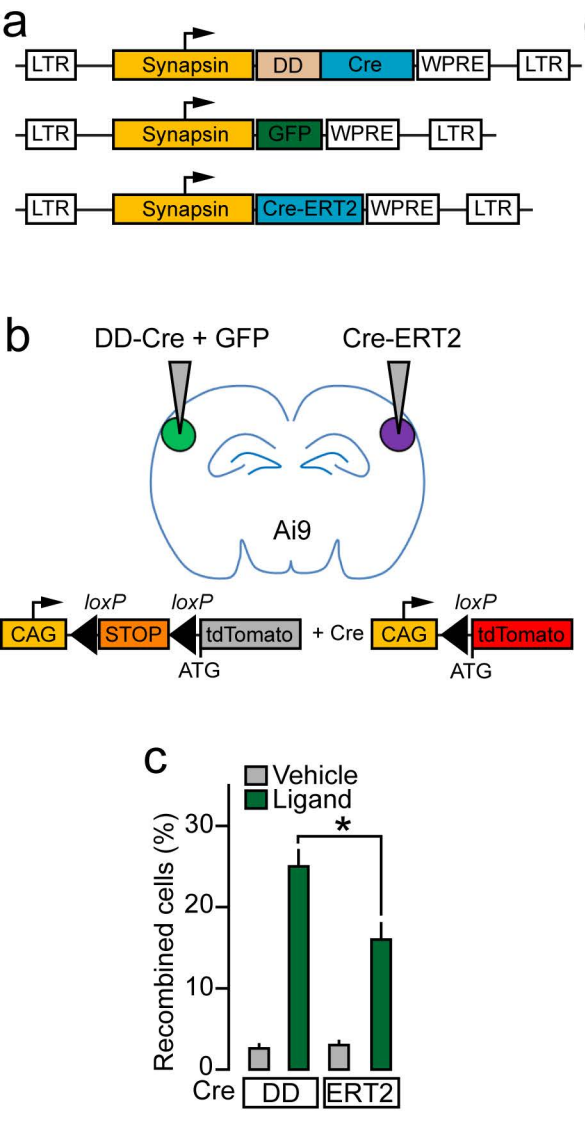

Supplementary Figure 4

a, Schematic representation of lentiviruses driving DD-Cre, Cre-ERT2 and GFP from neuronal Synapsin promoter.

b, Concentrated DD-Cre and Cre-ERT2 viruses of identical titers ($7x10^9$ GC/mL) were stereotactically injected into the left and right cortical hemispheres, respectively, of P1 Ai9 reporter mice (0.5µl total volume per injection). A small amount of constitutive GFP tracer virus was co-injected with DD-Cre to distinguish between hemispheres. Mice were than treated with either vehicle or drug mixture at P21 via intraperitoneal (i.p.) injection (170µg/gm TMP+100µg/gm Tamoxifen in corn oil) and analyzed by confocal imaging of brain sections at P28.

c and **d,** Quantitative analysis of constitutive and regulated DD-Cre and Cre-ERT2 activity. Note similar levels of background leak and significantly higher induction efficiency for DD-Cre. In panel c, data from 4-5 littermate pairs of mice are plotted as a percentage of DAPI-positive cells (Mean±S.E.M). * = $p<0.05$ (determined by Students t-test). See also Supplementary **Table 1.**

Supplementary Fig. 5

Developmental profile of CamKIIα promoter activity in the brain.

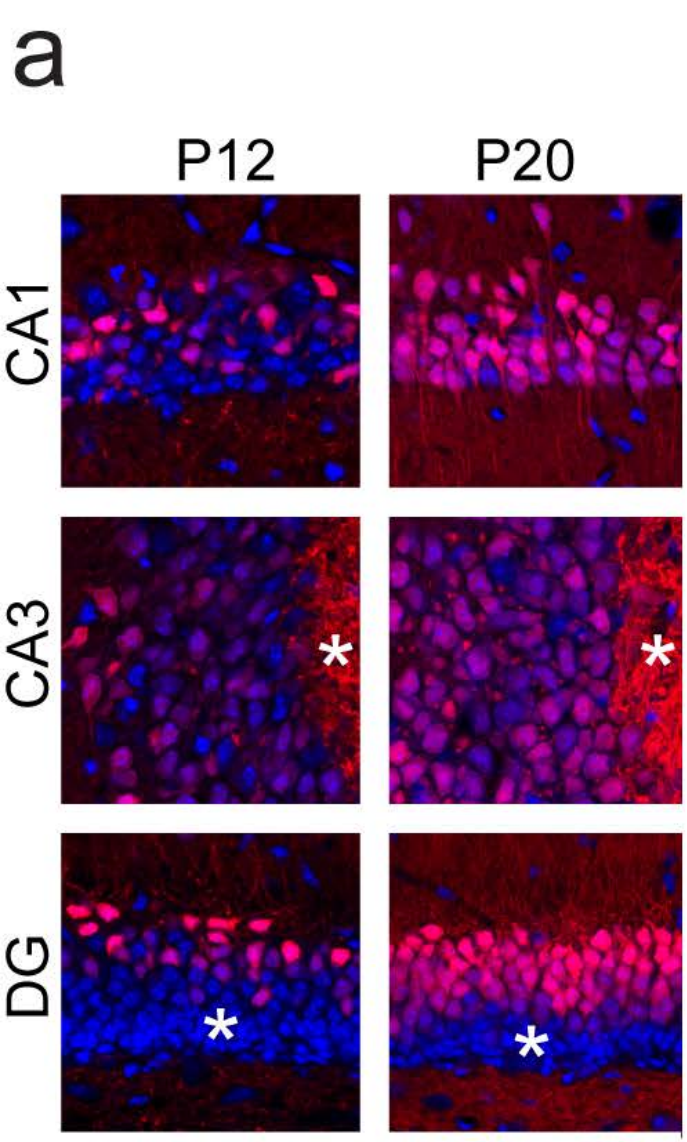

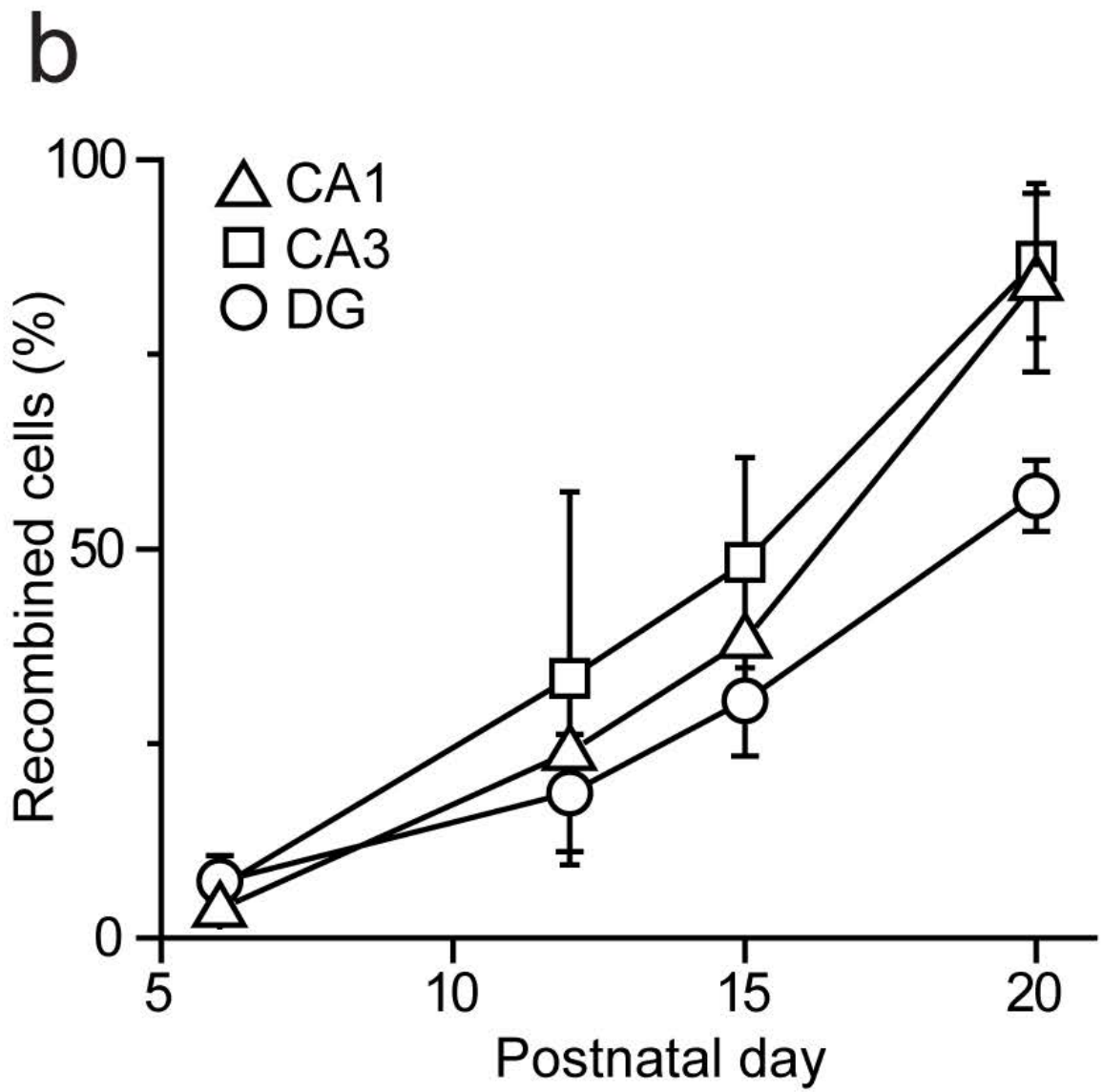

Supplementary Figure 5

Recombination was monitored with an Ai9 reporter in the brain of constitutive CamKIIα:Cre mice.

a, Typical images of DAPI-stained brain sections illustrate reporter induction in the hippocampal CA1, CA3 and DG regions at postnatal days 12 and 20 (P12 and P20). Note sparse expression at P12. Asterisks mark large mossy fiber presynaptic terminals in the CA3 region (middle) and differentiating CamKIIα-negative granule cells in the DG (bottom).

b, Quantification of recombination efficiency in the CA1, CA3 and DG at different time points of postnatal development.

Supplementary Fig. 6

Spatial pattern and efficiency of TMP-dependent recombination in the brain of DD-Cre/Ai9 mice.

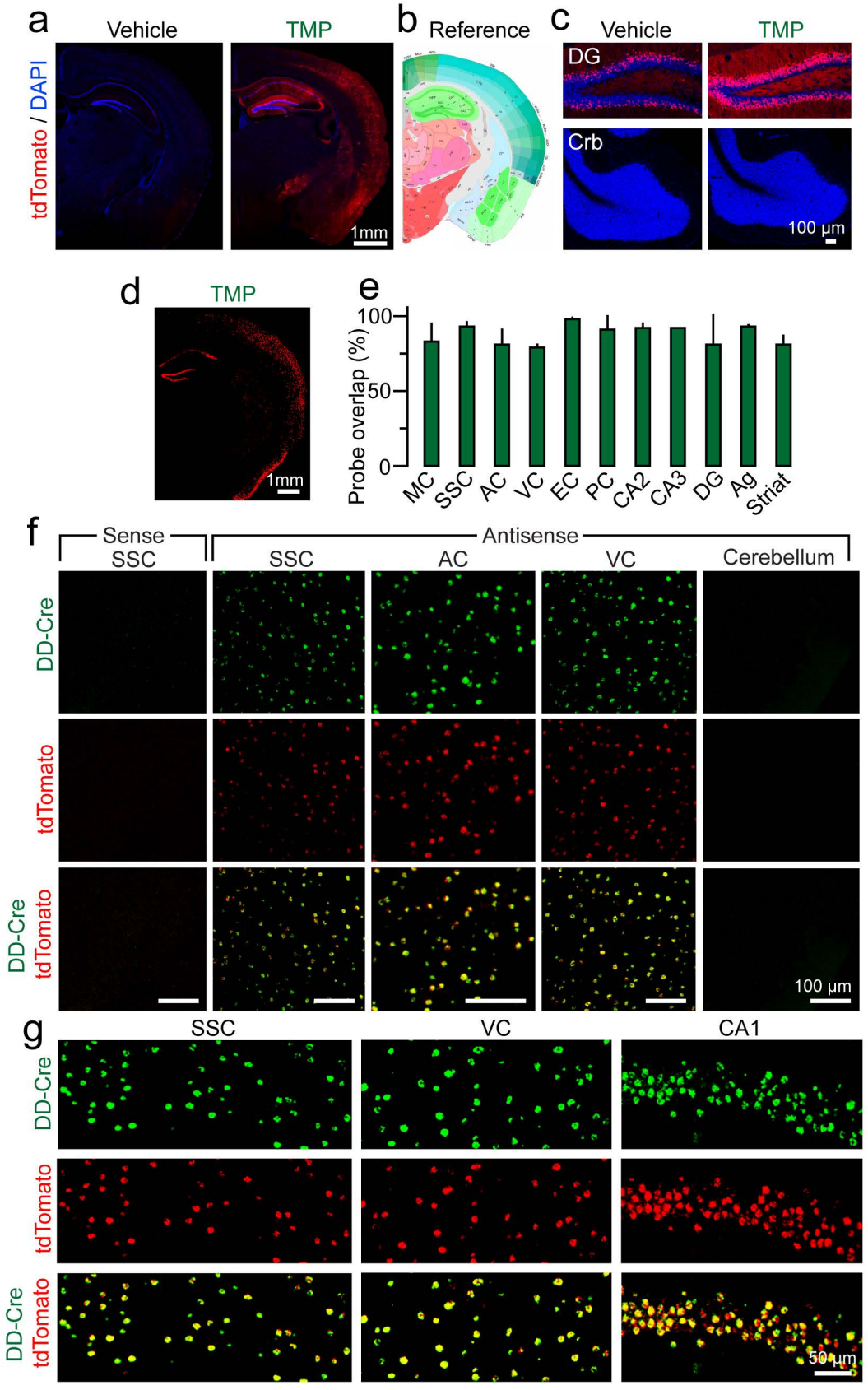

Supplementary Figure 6

Animals were injected at P30 with single vehicle and TMP doses (170 μg/gm), and analyzed at P37.

a and **b,** Representative images of coronal brain sections of vehicle- and TMP-mice mice and a corresponding reference map.

c, Enlarged images of DAPI-stained sections show reporter expression in the hippocampal Dentate Gyrus (DG) and lack of DD-Cre activity in cerebellum.

d-g, One TMP pulse induces recombination in the majority of neurons expressing DD-Cre mRNA. Brains of injected mice were analyzed by double situ hybridization with fluorescently labeled probes specific for DD-Cre and tdTomato.

d, Typical low-magnification image illustrates the global pattern of mRNA expression.

e, Analysis of co-expression of DD-Cre and tdTomato transcripts in various brain regions. MC=Motor cortex; SSC=Somatosensory cortex; AC=Auditory cortex; VC=Visual cortex; EC=Entorhinal cortex; PC=Piriform cortex; Ag=Amygdala. Data from 3-4 pairs of mice are represented as Mean±S.D.

f and **g,** Examples of high-magnification images used for quantifications and controls for in situ labeling specificity.

See also Supplementary **Table 1.**

Supplementary Fig. 7

Sparse TMP-dependent recombination in mosaic DD-Cre strain (LE-DD-Cre) enables tracing of individual neurons and synapses.

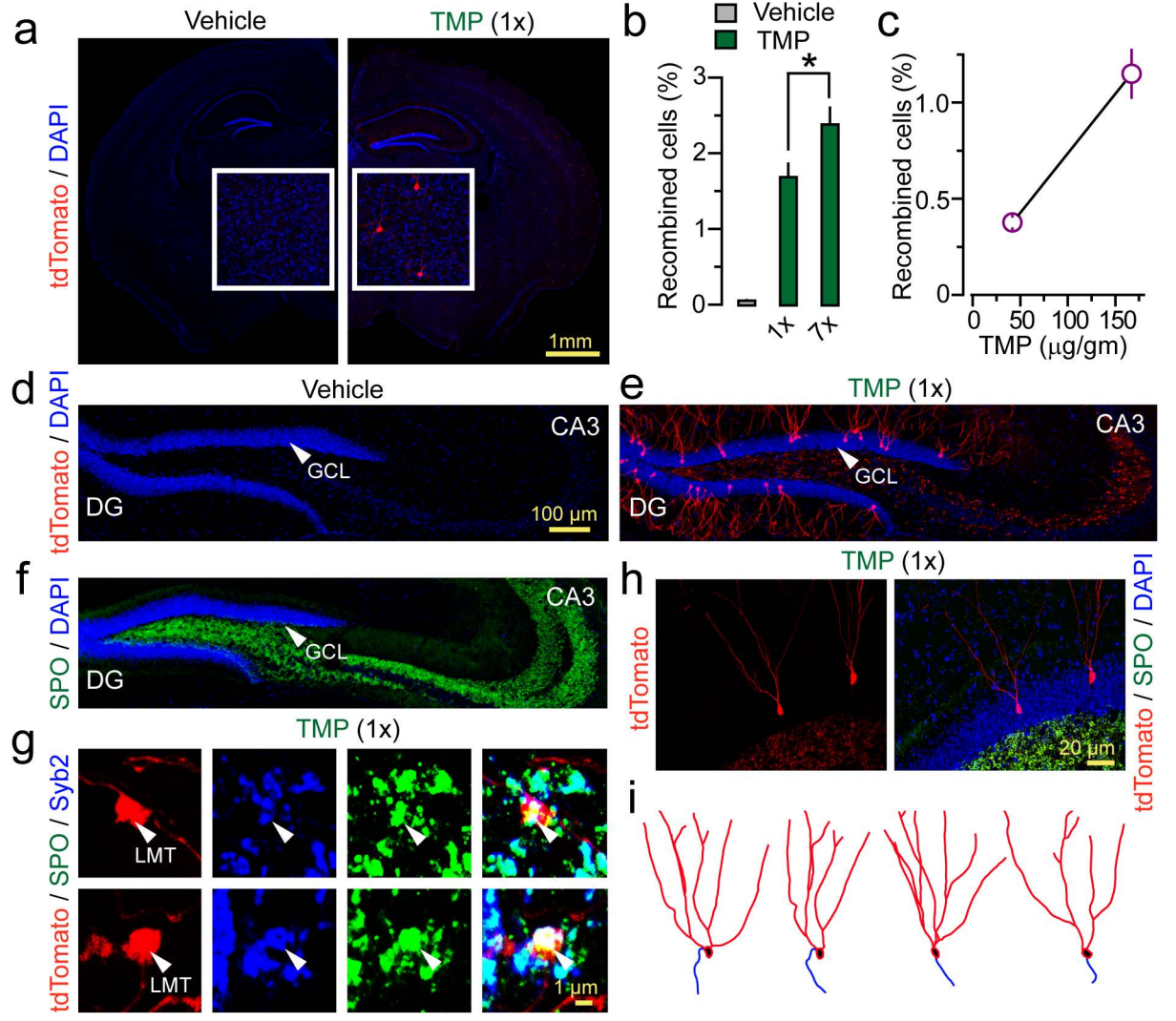

Supplementary Figure 7

a, Typical images of brain sections of P37 LE-DD-Cre/Ai9 mice that were injected with either vehicle or TMP (170 μg/gm) at P30. Enlarged images (inserts) show sparse TMP-inducible recombination in layers II-III of somatosensory cortex.

b and **c,** Efficiency and pharmacokinetics of recombination mediated by LE-DD-Cre in the DG.

b, Average densities of reporter-positive neurons in animals subjected to a single or seven sequential TMP doses (170 μg/gm daily).

c, TMP dose-response of DD-Cre activity. A single injection protocol was used.

d and **e,** Representative images show recombination of DG granule cells (GCs) in mice treated with a maximum TMP dose (170 μg/gm). The DAPI-positive neuronal cell bodies in the granule cell layer (GCL) are marked by arrows. The fine reporter-positive puncta observed in the Hilus and CA3 regions are GC axons and large presynaptic Mossy fiber terminals (LMTs).

f, Immunostaining for the native LMT-specific marker, Synaptoporin (SPO) reveals the distribution of GC synapses in the Hilus and CA3.

g, TMP-dependent tagging allows for LMT tracing. High-magnification images demonstrate the overlap of tdTomato-positive boutons formed by GC axons in the CA3 with synaptic puncta visualized by immunostaining for native SPO and Syb2.

h, Typical examples of individual GCs recombined in the DG of LE-DD-Cre/Ai9 mice in response to treatments with low TMP doses (50 μg/gm). Brain sections were stained with DAPI and an antibody to SPO.

i, Examples of three-dimensional reconstructions of dendritic trees of isolated GCs.

In panes b and c, each value was calculated in two animals and plotted as Mean±S.E.M. See also Supplementary **Table 1.**

Supplementary Fig. 8

Background DD-Cre activity depends on reporter copy numbers *in vivo*.

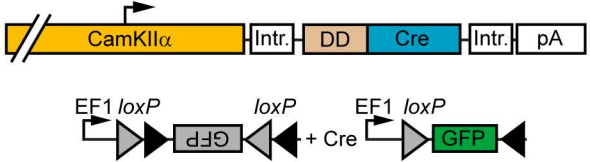

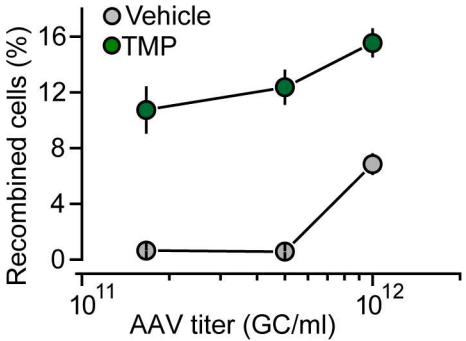

Supplementary Figure 8

P1 DD-Cre mice were injected into cortices with AAV2.5 DIO-GFP viruses of indicated titers. Animals were then treated with either vehicle or TMP (170 μg/gm) at P21 and analyzed for GFP expression at P28. Data from 2-3 littermate mice/group are plotted as a percentage of DAPI-positive cells (Mean±S.E.M). See also Supplementary **Table 1.**

Supplementary Fig. 9

Behavioral analysis of DD-Cre/TeNT mutants and their Cre-negative littermates.

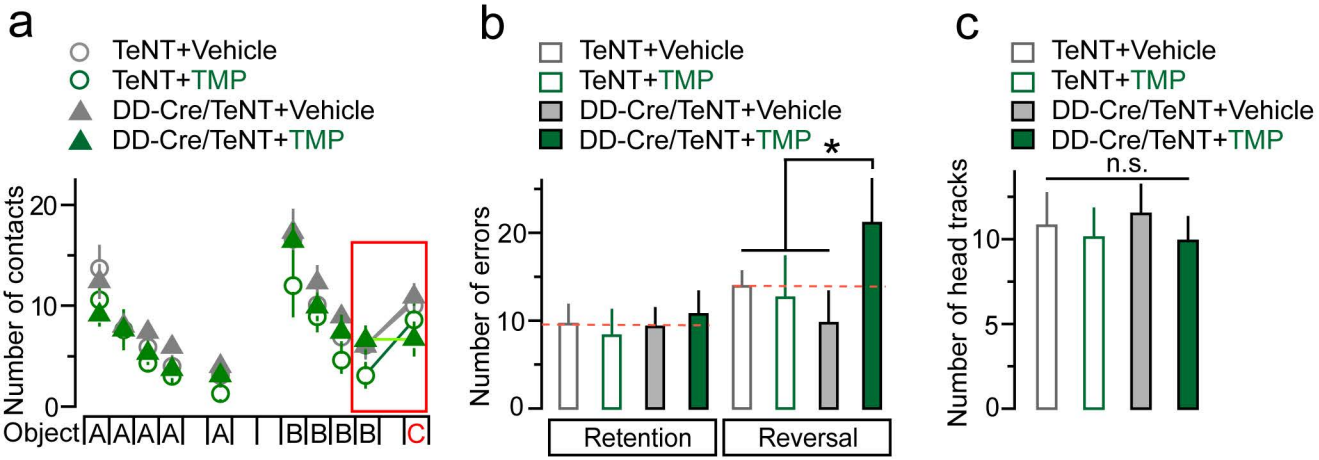

Supplementary Figure 9

Mice were treated with a single TMP dose (170 μg/gm) 48 hours prior to initiation of behavioral trials.

a and **b**, TMP-dependent neuronal silencing impairs recognition and spatial memory.

a, Averaged numbers of contacts made by animals with familiar (A and B) and novel objects (C).

b, Averaged numbers of errors made by animals in the Barnes maze retention and reversal tests.

c, All groups of mice have intact vision.

Data are represented as Mean±S.E.M. * = $p<0.05$ (defined by ANOVA). All measurements were performed with P60 animals. See also Supplementary **Table 3** for details.